Journal of Visualized Experiments

A Rat Model of Pressure Overload Induced Moderate Remodeling and Systolic Dysfunction as Opposed to Overt Systolic Heart Failure
--Manuscript Draft--

Article Type:	Invited Methods Article - JoVE Produced Video
Manuscript Number:	JoVE60954R1
Full Title:	A Rat Model of Pressure Overload Induced Moderate Remodeling and Systolic Dysfunction as Opposed to Overt Systolic Heart Failure
Section/Category:	JoVE Medicine
Keywords:	Rat, Pressure Overload, Hypertrophy, Heart Failure, Remodeling, Signal Transduction, Energetics, Metabolism, Calcium Cycling
Corresponding Author:	Antoine Chaanine, MD Tulane University School of Medicine New Orleans, LA UNITED STATES
Corresponding Author's Institution:	Tulane University School of Medicine
Corresponding Author E-Mail:	achaanine@tulane.edu
Order of Authors:	Antoine Chaanine, MD
	L. Gabriel Navar
	Patrice Delafontaine
Additional Information:	
Question	Response
Please indicate whether this article will be Standard Access or Open Access.	Standard Access (US$2,400)
Please indicate the **city, state/province, and country** where this article will be **filmed**. Please do not use abbreviations.	New Orleans, LA, Orleans county

1 **TITLE:**
2 **A Rat Model of Pressure Overload Induced Moderate Remodeling and Systolic Dysfunction as**
3 **Opposed to Overt Systolic Heart Failure**
4
5 **Authors and Affiliations:**
6 Antoine H. Chaanine[1], L. Gabriel Navar[2], Patrice Delafontaine[1,2,3]
7
8 [1]Department of Medicine/Heart and Vascular Institute, Tulane University, New Orleans, LA, USA
9 [2]Department of Physiology, Tulane University, New Orleans, LA, USA
10 [3]Department of Pharmacology, Tulane University, New Orleans, LA, USA
11
12 **Corresponding Author:**
13 Antoine H. Chaanine, MD
14 achaanine@tulane.edu
15
16 **Email addresses of Co-authors**
17 Patrice Delafontaine (pdelafon@tulane.edu)
18 L. Gabriel Navar (navar@tulane.edu)
19
20 **KEYWORDS:**
21 Rat, Pressure Overload, Hypertrophy, Heart Failure, Remodeling, Signal Transduction,
22 Energetics, Metabolism, Calcium Cycling
23
24 **SUMMARY:**
25 We describe the creation of a rat model of pressure overload induced moderate remodeling
26 and early systolic dysfunction where signal transduction pathways involved in the initiation of
27 the remodeling process are activated. This animal model will aid in identifying molecular targets
28 for applying early therapeutic anti-remodeling strategies for heart failure.
29
30 **ABSTRACT:**
31 In response to an injury, such as myocardial infarction, prolonged hypertension or a cardiotoxic
32 agent, the heart initially adapts through the activation of signal transduction pathways, to
33 counteract, in the short-term, for the cardiac myocyte loss and or the increase in wall stress.
34 However, prolonged activation of these pathways becomes detrimental leading to the initiation
35 and propagation of cardiac remodeling leading to changes in left ventricular geometry and
36 increases in left ventricular volumes; a phenotype seen in patients with systolic heart failure
37 (HF). Here, we describe the creation of a rat model of pressure overload induced moderate
38 remodeling and early systolic dysfunction (MOD) by ascending aortic banding (AAB) via a
39 vascular clip with an internal area of 2 mm^2. The surgery is performed in 200 g Sprague-Dawley
40 rats. The MOD HF phenotype develops at 8-12 weeks after AAB and is characterized
41 noninvasively by means of echocardiography. Previous work suggests the activation of signal
42 transduction pathways and altered gene expression and post-translational modification of
43 proteins in the MOD HF phenotype that mimic those seen in human systolic HF; therefore,
44 making the MOD HF phenotype a suitable model for translational research to identify and test

45   potential therapeutic anti-remodeling targets in HF. The advantages of the MOD HF phenotype
46   compared to the overt systolic HF phenotype is that it allows for the identification of molecular
47   targets involved in the early remodeling process and the early application of therapeutic
48   interventions. The limitation of the MOD HF phenotype is that it may not mimic the spectrum
49   of diseases leading to systolic HF in human. Moreover, it is a challenging phenotype to create,
50   as the AAB surgery is associated with high mortality and failure rates with only 20% of operated
51   rats developing the desired HF phenotype.
52

53   **INTRODUCTION:**
54   Heart failure (HF) is a prevalent disease and is associated with high morbidity and mortality[1].
55   Rodent pressure-overload (PO) models of HF, produced by ascending or transverse aortic
56   banding, are commonly used to explore molecular mechanisms leading to HF and to test
57   potential novel therapeutic targets in HF. They also mimic changes seen in human HF secondary
58   to prolonged systemic hypertension or severe aortic stenosis. Following PO, the left ventricular
59   (LV) wall gradually increases in thickness, a process known as concentric LV hypertrophy (LVH),
60   to compensate and adapt for the increase in LV wall stress. However, this is associated with the
61   activation of a number of maladaptive signaling pathways, which lead to derangements in
62   calcium cycling and homeostasis, metabolic and extracellular matrix remodeling and changes in
63   gene expression as well as enhanced apoptosis and autophagy[2-6]. These molecular changes
64   constitute the trigger for the initiation and propagation of myocardial remodeling and
65   transition into a decompensated HF phenotype.
66

67   Despite the use of inbred rodent strains and standardization of clip size and surgical technique,
68   there is tremendous phenotypic variability in LV chamber structure and function in aortic
69   banding models[7-9]. The phenotypic variability encountered after PO in rat, Sprague-Dawley
70   strain, is described elsewhere[10,11]. Of those, two HF phenotypes are encountered with evidence
71   of myocardial remodeling and activation of signal transduction pathways leading to a state of
72   heightened oxidative stress. This is associated with metabolic remodeling, altered gene
73   expression and changes in posttranslational modification of proteins, altogether playing a role
74   in the remodeling process[10,12]. The first is a phenotype of moderate remodeling and early
75   systolic dysfunction (MOD) and the second is a phenotype of overt systolic HF (HFrEF).
76

77   The PO model of HF is advantageous over the myocardial infarction (MI) model of HF because
78   the PO-induced circumferential and meridional wall stresses are homogeneously distributed
79   across all segments of the myocardium. However, both models suffer from variability in the
80   severity of PO[10,11] and in infarct size[13,14] along with intense inflammation and scarring at the
81   infarct site[15] as well as adhesion to the chest wall and surrounding tissues, which are observed
82   in the MI model of HF. Moreover, the rat PO induced HF model is challenging to create as it is
83   associated with high mortality and failure rates[10], with only 20% of the operated rats
84   developing the MOD HF phenotype[10].
85

86   The MOD is an attractive HF phenotype and constitutes an evolution of the traditionally created
87   HFrEF phenotype as it allows for early targeting of signal transduction pathways that play a role
88   in myocardial remodeling, especially when it pertains to perturbations in mitochondrial

89 dynamics and function, myocardial metabolism, calcium cycling and extracellular matrix
90 remodeling. These pathophysiological processes are highly evident in the MOD HF phenotype[11].
91 In this manuscript, we describe how to create the MOD and HFrEF phenotypes and we address
92 pitfalls while performing the ascending aortic banding (AAB) procedure. We also elaborate on
93 how to best characterize by echocardiography the two HF phenotypes, MOD and HFrEF, and
94 how to differentiate them from other phenotypes that fail to develop severe PO or that
95 develop severe PO and concentric remodeling but without significant eccentric remodeling.
96
97 **PROTOCOL:**
98
99 All methods and procedures described here have been approved by the Institutional Animal
100 Care and Use Committee (IACUC) of Tulane University School of Medicine.
101
102 **1.   Tools and instruments for AAB model creation**
103
104 1.1.   Obtain disinfectants, such as 70% isopropyl alcohol and povidone-iodine.
105
106 1.2. Obtain ketamine and xylazine for anesthesia and buprenorphine for analgesia.
107
108 1.3. Obtain a heating pad and heavy absorbency disposable underpad with the dimensions of
109 18 inches x 30 inches.
110
111 1.4. Obtain a 100% cotton twine roll, a tape and a hair clipper.
112
113 1.5. Obtain a 20 cm x 25 cm plastic board, thickness range between 3-5 mm.
114
115 1.6. Obtain a Z-LITE fiber optic illuminator.
116
117 1.7. Obtain a mechanical ventilator for small animals (e.g., SAR-830/AP).
118
119 1.8. Obtain 2-0 and 3-0 Vicryl taper sutures and nylon 3-0 monofilament suture, sterile gauze
120 pads and sterile extra large cotton tips and sterile gloves.
121
122 1.9. Obtain 16 G angiocath for intubation.
123
124 1.10. Purchase the following surgical tools.
125
126 1.10.1. Obtain a Weck stainless steel Hemoclip ligation and stainless-steel ligating clips.
127
128 1.10.2. Obtain hardened fine iris scissors.
129
130 1.10.3. Obtain Adson forceps.
131
132 1.10.4. Obtain two curved Graefe forceps.

133

134   1.10.5. Obtain a Halsted-Mosquito Hemostats-straight forceps.

135

136   1.10.6. Obtain a Mayo-Hegar needle holder.

137

138   1.10.7. Obtain an Alm chest retractor with blunt teeth.

139

140   1.11. Utilize and obtain an autoclave and a bead sterilizer.

141

142   **2.   Ascending aortic banding surgical procedure**

143

144   2.1.   Anesthetize the animal with an intraperitoneal injection of 65 mg/kg ketamine and 5
145   mg/kg xylazine.

146

147   NOTE: Allow a few minutes for the animal to be completely sedated and flaccid. If the
148   anesthetic dose is not sufficient and the animal is still moving in the cage, re-inject the animal
149   with the same anesthetic dose after allowing enough time, around 5-10 minutes between
150   subsequent injections. Most animals require 1-2 injections to achieve deep sedation and
151   anesthesia.

152

153   2.2.   Shave the hair on the surgical site located at the right lateral thoracic area under the
154   right armpit.

155

156   2.3.   Stabilize the animal by gently taping all four limbs to the plastic board. Then perform
157   endotracheal intubation with a 16 G angiocath. After the animal is successfully intubated,
158   initiate mechanical ventilation with tidal volumes of 2 mL at 50 cycles/min and FiO_2 of 21%.
159   Look for the symmetrical rise in chest wall with each breath.

160

161   2.4.   Turn the animal slowly to lie on its left lateral side, and then bend the tail in a U-shape
162   manner and stabilize it by gently taping it to the plastic board. Then go ahead and disinfect the
163   shaved area with topical application of povidone-iodine.

164

165   2.5.   Perform a right horizontal skin incision, 1-2 centimeters long, in the right axillary area 1
166   cm below the right armpit. Then, dissect the thoracic muscular layer until reaching the thoracic
167   rib cage. Make a 1 cm thoracotomy between the 2nd and 3rd rib cage.

168

169   2.5.1. While dissecting the muscular layer of the chest, be careful and avoid injury of the right
170   axillary artery, which runs underneath the right armpit.

171

172   NOTE: Thoracotomy performed between the 1st and the 2nd rib carries the risk of banding the
173   right brachiocephalic artery instead of the ascending aorta. Thoracotomy between the 3rd and
174   the fourth rib makes it hard to visualize and band the ascending aorta, as the operator will be
175   looking at the right atrium.

176

NOTE: Avoid extending the thoracotomy too medially towards the sternum to avoid dissecting and injuring the right internal mammary artery.

2.6.   Dissect the two lobes of the thymus gland gently and push them apart on the side. Then identify the ascending aorta and isolate it from the superior vena cava by blunt dissection via a curved Graefe forceps.

NOTE: Significant manipulation of the thymus gland will render it swollen and makes it hard to visualize the ascending aorta.

2.6.1. Dissect the superior vena cava from the aorta with extra caution to avoid injury or rupture of the superior vena cava, which is fatal. This may be the trickiest part of the procedure and is expected to happen from time to time even in most experienced hands, but often with beginners and learners.

2.7.   Lift gently the ascending aorta with a curved Graefe forceps and place the vascular clip around the ascending aorta.

2.7.1. Adjust the vascular hemoclip ligation tool via a plastic pre-cut 7" piece to obtain a vascular clip of the desired internal area of 1.5 mm^2 or 2 mm^2, depending on which HF model is desired.

2.8.   Suture the thorax via a Vicryl 2-0 monofilament suture. Then suture the muscular layer of the chest via a 3-0 Vicryl taper suture. Then suture the skin incision via a Nylon 3-0 monofilament suture.

2.9.   Administer subcutaneous injection of 0.6 – 1 mg/kg buprenorphine SR.

NOTE: Leave the animal to recover on a heating pad under regular monitoring. Once the animal shows signs of recovery from anesthesia (able to breath spontaneously - without evidence of gasping or use of accessory muscles for more than two minutes - and has good reflexes, red and warm extremities), extubate the animal and return it to the cage.

3.   Echocardiography

3.1.   Sedate the animal with intraperitoneal injection of 80-100 mg/kg ketamine. Ensure adequate sedation for proper acquisition of good quality echo images.

NOTE: The use of isoflurane as an anesthetic is discouraged for its cardiodepressor effect, especially in the setting of severe pressure overload and might give a false impression of LV dilatation and systolic dysfunction that resolves once animal is off anesthetic.

3.1.1. Be cautious and administer half or even one third of the dose of ketamine in animals that look dyspneic and tachypneic with suspicion that they have developed the HFrEF

221 phenotype.

222

223 3.2.   Shave the hair of the chest, anteriorly, in the completely sedated animal.

224

225 3.3.   Lay the animal on its back and stabilize it to the plastic board.

226

227 3.4.   Acquire 2D parasternal long axis and 2D parasternal short axis view clips at the level of
228 the papillary muscle. Also, obtain M-mode images from the short parasternal axis view at the
229 level of the papillary muscle to measure LV septal and posterior wall thickness in diastole as
230 well as LV end-diastolic and end-systolic diameter.

231

232 3.4.1. Acquire images or clips at a heart rate of 370 - 420 beats per minute to ensure proper
233 assessment of LV size and function. Acquisition of images at lower heart rates will lead to a
234 false impression of depressed LV function and LV dilatation.

235

236 NOTE: Acquisition of foreshortened 2D long parasternal axis view images/clips lead to false
237 measurements. For quality control purposes, make sure that the LV apex and the aorto-mitral
238 angle are visualized within the same plane cut.

239

240 3.4.2. Acquire 2D short parasternal axis view images/clips at the level of the mid papillary
241 muscle. This will serve as a reference to obtain reliable serial and subsequent LV measurements
242 while following the animals over time throughout the study period.

243

244 3.5. Obtain M-mode images in long parasternal axis view at the level of the aortic valve to
245 assess the relative aortic to left atrium (LA) diameter at end systole.

246

247 NOTE: Animals with the MOD and HFrEF phenotypes should show evidence of LA dilatation
248 with LA/Ao ratio being ≥1.25 and <1.5 in MOD HF phenotype and ≥1.5 in the HFrEF
249 phenotype[10].

250

251 **REPRESENTATIVE RESULTS:**
252 Characterization of the HF phenotypes, that develop 8-12 weeks following AAB, could be easily
253 performed via echocardiography. Representative M-mode images of Sham, Week 3 post-AAB,
254 MOD and HFrEF phenotypes are presented in **Figure 1A**. **Figure 1B** and **Figure 1C** are showing
255 the vascular clip size for the creation of the MOD HF phenotype and HFrEF phenotype,
256 respectively. The LV end-diastolic (LVEDV) and end-systolic (LVESV) volumes could be calculated
257 by using the formulae of the area length method: $V=5/6 \times A \times L$, where V is the volume in ml; A is
258 the cross sectional area of the LV cavity in cm^2, obtained from the short parasternal axis view at
259 the level of the mid-papillary muscle in diastole (Ad) and in systole (As); and L is the length of
260 the LV cavity in cm, measured from the long parasternal axis view as the distance from the
261 endocardial LV apex to the mitral-aortic junction in diastole (Ld) and in systole (Ls).
262 Representative 2D long parasternal axis and short parasternal axis echocardiography images,
263 with illustration on how to measure Ld, Ls, Ad and As, in Sham and MOD HF phenotype are
264 presented in **Figure 2**. The LVEDV in the MOD HF phenotype usually ranges between 600 – 700

μL, with very few animals having LVEDV greater than 700 μL and up to 1000 μL; whilst, the LVESV in the MOD phenotype ranges between 120 – 160 μL (**Table 1**). From the 2D short parasternal axis view echocardiography images presented in **Figure 2**, one could appreciate the degree of LVH in the MOD phenotype compared to the sham. Representative pressure-volume loop tracings of the Sham, Week 3 post-AAB, MOD and HFrEF phenotypes are presented in **Figure 3**. The LV maximum pressure is at least 200 mmHg, even at week 3 post-AAB, and increases further at week 8 post-AAB due to the mismatch between the growth of the animal and aorta and the fixed created stenosis in the ascending aorta. Note that the animals at week 3 post-AAB are fully compensated with shift of the LVEDV and LVESV to the left compared to the sham. With progressive eccentric hypertrophy and remodeling, there is a shift in LVEDV and LVESV to the right in the MOD and HFrEF phenotypes compared to week 3 post-AAB. One could appreciate also the significant increase in LVESV in the MOD phenotype and the profound increase in LVESV in the HFrEF phenotype, which reflects the significant and profound decreases in stroke volume and LVEF in the MOD and HFrEF phenotypes, respectively, compared to week 3 post-AAB. Moreover, one could appreciate the significant increase in LVEF at week 3 post-AAB and the significant decrease in LVEF in the HFrEF phenotype compared to the sham.

The rat PO induced HF model is associated with high mortality and failure rates. Only about 20% of the rats that undergo AAB, with a vascular clip of 2 mm^2 in internal diameter, will transition to develop the MOD HF phenotype. Representative M-mode images of the failed phenotypes are presented in **Figure 4**. **Figure 4A** is showing representative M-mode images of animals that did not develop LVH at week 8 post-AAB, and had completely lost the PO with complete regression of LVH (sham-like) or had variable degree of LVH and PO at week 8 post-AAB causing a mild-moderate LVH phenotype. The second failed phenotype group is presented in **Figure 4B** showing representative M-mode images of animals with severe PO (LV maximum pressure >200 mmHg) and severe LVH who remained compensated with no evidence of eccentric remodeling, concentric remodeling (CR) group, or with a mild (MILD group) eccentric remodeling. Echocardiography and hemodynamic data of the sham, failed, and successful/desired phenotypes are presented in **Figure 5** and **Table 1**. Note the progressive increases in heart weight and LV weight as the animals transition from a compensated phenotype to a more eccentric and remodeled phenotype. Also, there is an exponential increase in LVESV and decrease in LVEF as the animals transition from a compensated concentric remodeling to a decompensated eccentrically remodeled phenotype. Of particular interest is that both the MOD and HFrEF HF phenotypes have a similar degree of myocardial stiffness as measured by the stiffness-coefficient β of the end-diastolic pressure volume relationship (EDPVR (mmHg/μL)) compared to all the other phenotypes, whereas there is a gradual decrease in LV efficiency as the animals transition to a more eccentrically remodeled phenotype. LV efficiency is calculated from the end-systolic pressure volume relationship (ESPVR) divided by the arterial elastance (EA). Despite that there is no significant statistical difference in ESPVR and ESPVR/EA between the MOD and HFrEF phenotypes and the sham group, this is falsely the case as the MOD and HFrEF phenotypes have a significantly higher LV end-systolic pressure compared to the sham, making the ESPVR slope falsely steeper with shift in V0 to the right compared to the sham. Moreover, when the MOD and HFrEF phenotypes are

309 compared to the compensated and concentrically remodeled phenotypes, which have the same
310 degree of PO, then one could appreciate the significant and progressive increase in LVESV and
311 drop in ESPVR and ESPVR/EA with progressive eccentric remodeling, as observed in the MOD
312 and HFrEF phenotypes compared to the CR and MILD phenotypes (**Figure 5** and **Table 1**).
313
314 **FIGURE AND TABLE LEGENDS:**
315 **Figure 1. Representative heart failure phenotypes at week 8 following ascending aortic**
316 **banding.** (**A**) Representative M-mode images of sham animals, animals three weeks following
317 ascending aortic banding (AAB) and eight weeks following AAB. Figure 1A has been modified
318 from Chaanine et al., American Journal of Physiology-Heart and Circulatory physiology, 2016.
319 (**B**) Vascular clip size for the creation of severe left ventricular hypertrophy (LVH) with moderate
320 eccentric remodeling (MOD). (**C**) Vascular clip size for the creation of severe LVH with overt
321 systolic heart failure (HFrEF). Figures 1B and 1C has been obtained and modified from Chaanine
322 et al., Methods in Molecular Biology, 2018.
323
324 **Figure 2. Calculation of left ventricular volumes by echocardiography using the area-length**
325 **method.** Representative 2D long parasternal and 2D short parasternal axis view
326 echocardiography images to measure left ventricular (LV) cavity length in diastole (Ld) and in
327 systole (Ls) and LV cavity cross sectional area in diastole (Ad) and in systole (As) in order to
328 calculate LV volumes at end of diastole and systole.
329
330 **Figure 3. Pressure-volume loop tracings were obtained via a 1.9 F rat pressure-volume**
331 **catheter using the open chest and left ventricular apical puncture approach.** Representative
332 pressure-volume loop tracings in Sham, week 3 following AAB, MOD and HFrEF phenotypes at
333 week 8 following AAB. Figure has been modified from Chaanine et al., Circulation: Heart Failure,
334 2013.
335
336 **Figure 4. Encountered phenotypes at week 8 following AAB with failure to develop the**
337 **desired heart failure phenotype(s).** (**A**) Representative M-mode images of animals that lost the
338 pressure overload (PO) and did not develop LVH (Sham-like) and those with variable PO and
339 LVH (mild-moderate LVH) phenotypes. (**B**) Representative M-mode images of animals that
340 developed severe PO, LVH and concentric remodeling (CR), but without (CR) or with mild
341 (MILD) eccentric remodeling phenotypes. Figure 4B has been modified from Chaanine et al.,
342 Journal of American Heart Association, 2017.
343
344 **Figure 5. Echocardiography and pressure-volume loop parameters in the different**
345 **phenotypes.** Data are presented as individual values (dots) with median (horizontal line) in the
346 different phenotypes at week 8 post-AAB. Statistical analysis results of the presented data in
347 the different phenotypes are shown in table 1. LVESV: left ventricular end-systolic volume,
348 LVEF: left ventricular ejection fraction, EDPVR: end-diastolic pressure volume relationship,
349 ESPVR: end-systolic pressure volume relationship, EA: arterial elastance.
350
351 **Table 1. Echocardiography and pressure-volume parameters in Sham, Sham-like, Mild-**
352 **moderate LVH, CR, MILD, MOD and HFrEF phenotypes.**

353
354 **DISCUSSION:**
355 Following PO related to AAB in rat, the LV undergoes concentric remodeling by increasing LV
356 wall thickness, known as concentric LVH, as a compensatory mechanism to counteract for the
357 increase in LV wall stress. Increase in LV wall thickness becomes noticeable during the first
358 week following AAB and reaches its maximum thickness at 2-3 weeks post-AAB. During this
359 time period, activation of maladaptive signal transduction pathways lead to progressive
360 enlargement of the LV with increases in LV volumes, a process known as eccentric hypertrophy
361 or remodeling. It is expected that the HF phenotype in rat develops around 8 weeks following
362 AAB in most of the animals with few of them developing HF at week 12 following AAB. Two HF
363 phenotypes ensue depending on the severity of AAB. The MOD phenotype is obtained via the
364 creation of ascending aortic banding (AAB) with a vascular clip of 2 mm^2 in internal diameter,
365 whilst, the creation of the HFrEF phenotype requires AAB with a tighter vascular clip of 1.5 mm^2
366 in internal diameter. It is important to perform echocardiography at 2-3 weeks following
367 ascending aortic banding to verify the presence of severe concentric LVH. Severe LVH is defined
368 as LV septal and posterior wall thickness ≥1.5 times normal (0.19 cm), and usually ranges
369 between 0.27 – 0.3 cm. Animals that do not develop severe LVH at week 3 following AAB, will
370 be deemed as having unsuccessful AAB and should not be followed thereafter. Those that have
371 developed severe LVH at week 3 following AAB, will undergo echocardiography at week 8
372 following AAB to assess for the development of the desired HF phenotype. It is not rare to
373 encounter animals that had severe LVH at week 3 following AAB to have regression or
374 resolution of LVH at week 8 following AAB, for reasons that we will address in the latter section
375 of the discussion. Animals with severe LVH and concentric remodeling without or with mild
376 eccentric remodeling at week 8 following AAB, therefore the CR and MILD phenotypes,
377 respectively, are unlikely to develop further eccentric remodeling even if they are followed for
378 an extended month or two. Those that are in between the MILD and MOD phenotype, may
379 develop the MOD HF phenotype if they are followed for one more month.
380
381 The PO rat model can be frustrating due to the associated high mortality and failure rates[10],
382 despite use of a standardized vascular clip size and surgical technique, which also adds to the
383 research expense, due to the large number of animals that need to undergo AAB in order to
384 achieve the desired target number (n), and the length of time that the animals need to be
385 followed before they develop the desired HF phenotype. Failure to develop severe LVH is
386 related to either unsuccessful banding or banding of the right brachiocephalic artery instead of
387 the aorta, which is not uncommon. Regression and/or resolution of severe LVH in subsequent
388 follow up assessments is related to aneurysm formation and peri-band aortic remodeling that
389 leads to loss in the severity of PO[9]. It remains unclear why animals with severe LVH and PO
390 develop phenotypic variability in regard to eccentric remodeling despite having the same clip
391 size, sex and strain. It is recommended to visualize the ascending aorta to screen for peri-band
392 aortic remodeling and aneurysmal formation. Animals that develop ascending aortic aneurysm
393 ≥1 cm in diameter should be euthanized, as this will cause dyspnea and distress to the animal
394 due to impingement on surrounding structures. Also, it is recommended to check for turbulent
395 flow across the band by color Doppler, but unfortunately precise estimation of pressure
396 gradient across the band by continuous Doppler is not feasible due to the inability to align the

397   continuous Doppler with the blood flow direction in the ascending aorta.
398

399   The MOD is an attractive HF phenotype and constitutes an evolution of the traditionally created
400   HFrEF phenotype as it allows for targeting of signal transduction pathways that play role in
401   myocardial remodeling early on in the disease process, especially when it pertains to
402   perturbations in mitochondrial dynamics and function, myocardial metabolism and calcium
403   cycling and extracellular matrix remodeling and myocardial stiffness; features that are highly
404   evident in the MOD HF phenotype[11]. Also, the early postoperative mortality (defined as
405   mortality in the first 7 days post-AAB) is lower with the clip size of 2 mm^2, for the creation of
406   MOD phenotype, than the clip size of 1.5 mm^2, for the creation of HFrEF phenotype[10], (5% vs
407   21%, P = 0.009 using Fisher's exact test). However, the success rate between the two clip sizes,
408   for the creation of MOD and HFrEF phenotypes, is not statistically significant[10], (20% vs 13%, P =
409   0.56 using Fisher's exact test). Moreover, the aortic banding by vascular clip is advantageous
410   over the aortic banding by tightening a nylon suture against a 27 G needle, a technique often
411   used to constrict the transverse aorta in mice, because there is less variation in clip size and less
412   trauma to the aorta compared to the suture technique.
413

414   The PO model of HF is advantageous over the myocardial infarction (MI) model of HF because
415   the PO-induced circumferential and meridional wall stress is homogeneously distributed across
416   all segments of the myocardium. However, both models suffer from variability in the severity of
417   PO[10,11] and in infarct size[13,14] along with intense inflammation and scarring at the infarct site[15]
418   as well as adhesion to the chest wall and surrounding tissues observed in the MI model of HF.
419   Moreover, the rat PO induced HF model is challenging to create as it is associated with high
420   mortality and failure rates[10], with only 20% of the operated rats developing the MOD HF
421   phenotype[10]. When compared to the spontaneously hypertensive rat (SHR) model, the PO-
422   induced HF model is a better model to study pathways related to myocardial remodeling. The
423   increase in afterload and myocardial wall stress in systole is much higher in the PO-induced HF
424   model than the SHR model. It takes about two years for the SHR to develop systolic HF and the
425   mechanism of systolic HF is not entirely known and is confounded by aging[16]. The SHR model
426   and other models of hypertension, such as the DOCA salt model, are more frequently used to
427   investigate mechanisms and therapies related to hypertension and possibly diastolic
428   dysfunction[16].
429

430   In conclusion, the MOD HF phenotype is an attractive model to study signal transduction
431   pathways in the context of myocardial remodeling and can be utilized for application and
432   testing of potential therapeutic strategies, before validation of their efficacy in large animal
433   models and in human heart failure.
434

437

438   **DISCLOSURES:**
439   All authors report no conflict of interest.
440

REFERENCES:

1   McMurray, J.J., Petrie, M.C., Murdoch, D.R., Davie, A.P. Clinical epidemiology of heart failure: public and private health burden. *European Heart Journal.* **19 Suppl P**, P9-16 (1998).

2   Berk, B.C., Fujiwara, K., Lehoux, S. ECM remodeling in hypertensive heart disease. *Journal of Clinical Investigation.* **117** (3), 568-575 (2007).

3   Frey, N., Olson, E.N. Cardiac hypertrophy: the good, the bad, and the ugly. *Annual Review of Physiology.* **65**, 45-79 (2003).

4   Hill, J.A., Olson, E.N. Cardiac plasticity. *New England Journal of Medicine.* **358** (13), 1370-1380 (2008).

5   Kehat, I., Molkentin, J.D. Molecular pathways underlying cardiac remodeling during pathophysiological stimulation. *Circulation.* **122** (25), 2727-2735 (2010).

6   Rothermel, B.A., Hill, J.A. Autophagy in load-induced heart disease. *Circulation Research.* **103** (12), 1363-1369 (2008).

7   Barrick, C.J. et al. Parent-of-origin effects on cardiac response to pressure overload in mice. *American Journal of Physiology-Heart and Circulatory Physiology.* **297** (3), H1003-1009 (2009).

8   Barrick, C.J., Rojas, M., Schoonhoven, R., Smyth, S.S.,, Threadgill, D.W. Cardiac response to pressure overload in 129S1/SvImJ and C57BL/6J mice: temporal- and background-dependent development of concentric left ventricular hypertrophy. *American Journal of Physiology-Heart and Circulatory Physiology.* **292** (5), H2119-2130 (2007).

9   Lygate, C.A. et al. Serial high resolution 3D-MRI after aortic banding in mice: band internalization is a source of variability in the hypertrophic response. *Basic Research in Cardiology.* **101** (1), 8-16 (2006).

10   Chaanine, A.H., Hajjar, R.J. Characterization of the Differential Progression of Left Ventricular Remodeling in a Rat Model of Pressure Overload Induced Heart Failure. Does Clip Size Matter? *Methods in Molecular Biology (Clifton, N.J.).* **1816**, 195-206 (2018).

11   Chaanine, A.H. et al. Mitochondrial Integrity and Function in the Progression of Early Pressure Overload-Induced Left Ventricular Remodeling. *Journal of the American Heart Association.* **6** (6) (2017).

12   Chaanine, A.H. et al. Potential role of BNIP3 in cardiac remodeling, myocardial stiffness, and endoplasmic reticulum: mitochondrial calcium homeostasis in diastolic and systolic heart failure. *Circulation: Heart Failure.* **6** (3), 572-583 (2013).

13   Takagawa, J. et al. Myocardial infarct size measurement in the mouse chronic infarction model: comparison of area- and length-based approaches. *Journal of Applied Physiology (Bethesda, Md. : 1985).* **102** (6), 2104-2111 (2007).

14   Vietta, G.G. et al. Early use of cardiac troponin-I and echocardiography imaging for prediction of myocardial infarction size in Wistar rats. *Life Sciences.* **93** (4), 139-144 (2013).

15   Frangogiannis, N.G. The inflammatory response in myocardial injury, repair, and remodelling. *Nature Reviews. Cardiology.* **11** (5), 255-265 (2014).

16   Doggrell, S.A., Brown, L. Rat models of hypertension, cardiac hypertrophy and failure. *Cardiovascular Research.* **39** (1), 89-105 (1998).
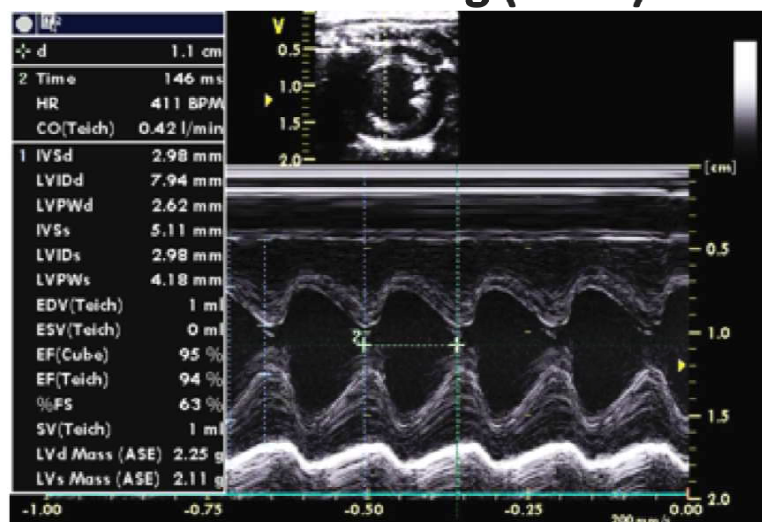
Figure 1   Click here to access/download;Figure;Figure 1.eps ⬇

A

Representative HF phenotype of moderate eccentric remodeling compared to overt systolic heart failure
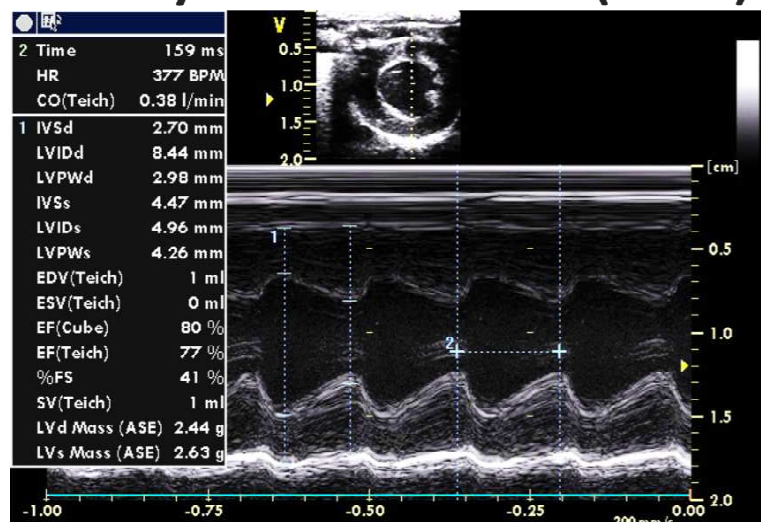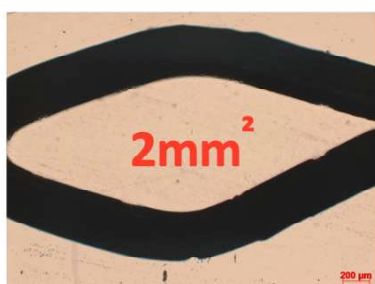
Sham

Week 3 post-AAB
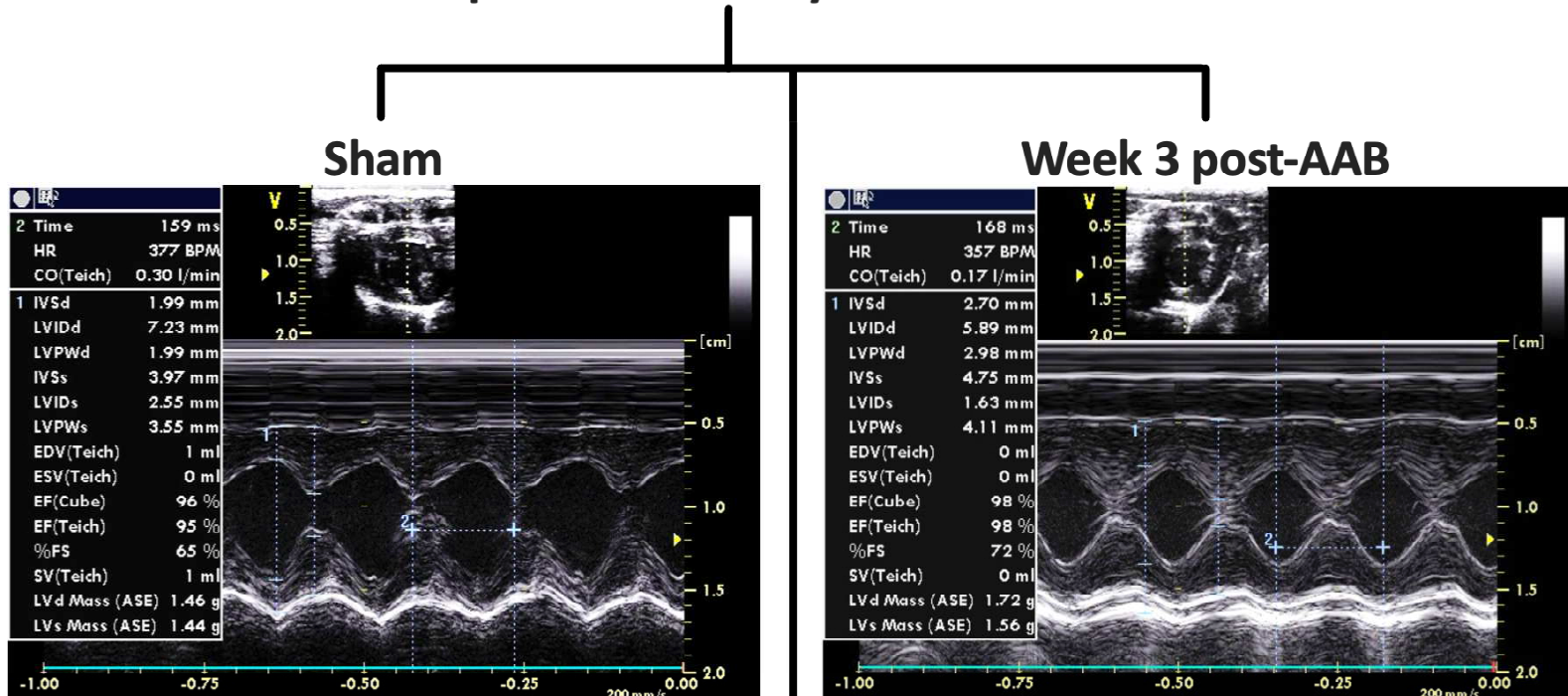
Week 8 post-AAB

Severe LVH and moderate eccentric remodeling (MOD)

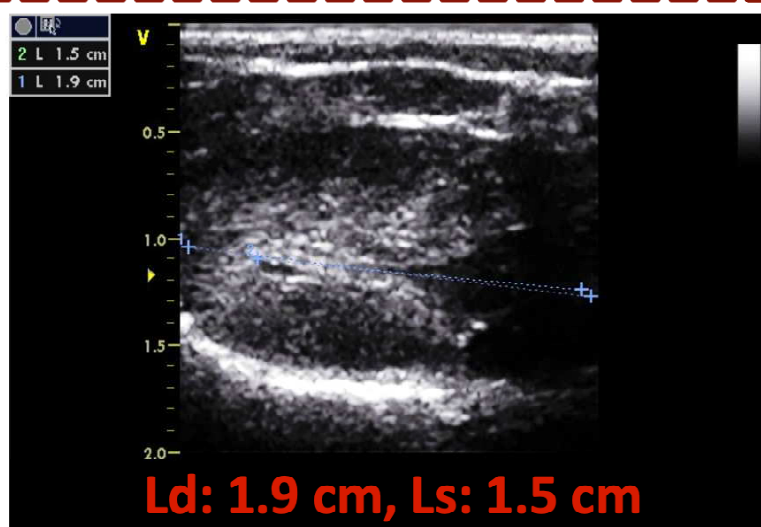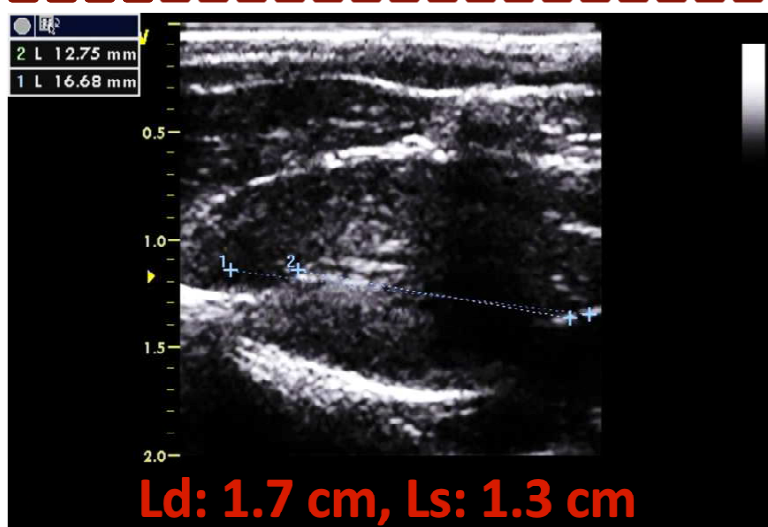### Severe LVH and transition to overt systolic heart failure (HFrEF)

Figure 2
Click here to access/download;Figure;Figure 2.eps ⬇

Calculation of LV volumes by echocardiography using the area-length method

Sham

Severe LVH and moderate eccentric remodeling (MOD)
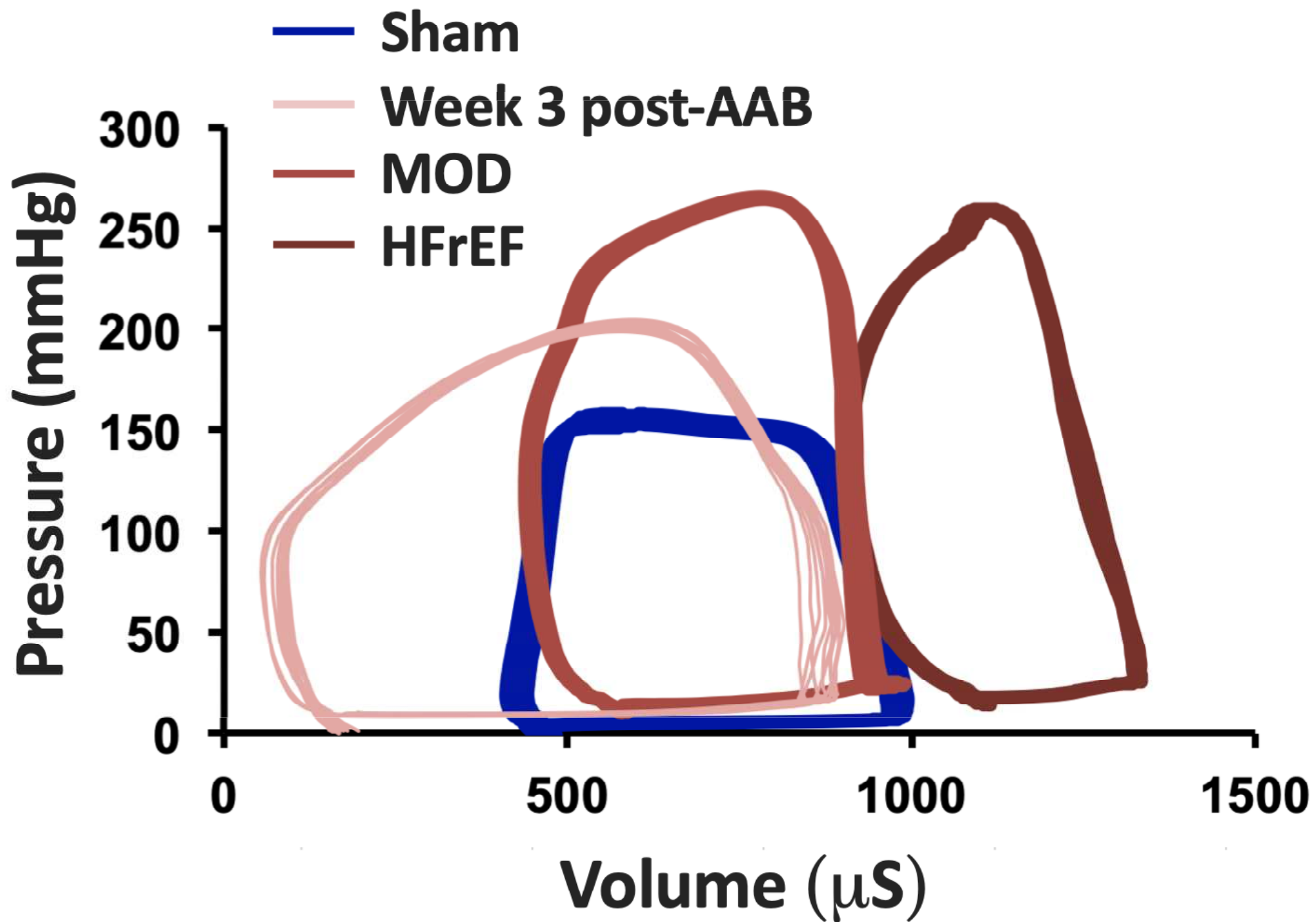
Long Parasternal axis view

Ld: 1.7 cm, Ls: 1.3 cm

Ld: 1.9 cm, Ls: 1.5 cm

Measurement of LV cavity length at end-diastole (Ld) and end-systole (Ls)

Short Parasternal axis view

Ad: 0.43 cm^2, As: 0.12 cm^2

Ad: 0.64 cm^2, As: 0.15 cm^2
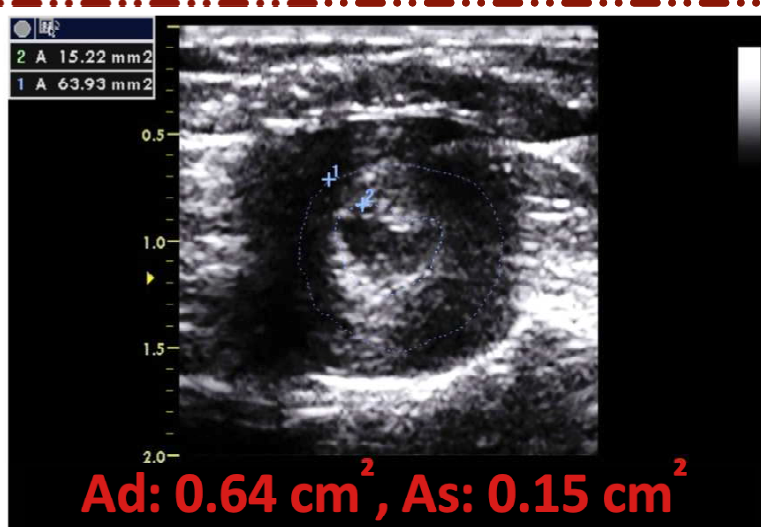
Measurement of LV cavity area at end-diastole (Ad) and end-systole (As)

Figure 3

Click here to access/download;Figure;Figure 3.eps ⬇

Figure 4   Click here to access/download;Figure;Figure 4.eps ⬇

A

Animals that failed to develop severe LVH and severe pressure overload at week 8 post-AAB

Sham-like   **Mild - moderate LVH**
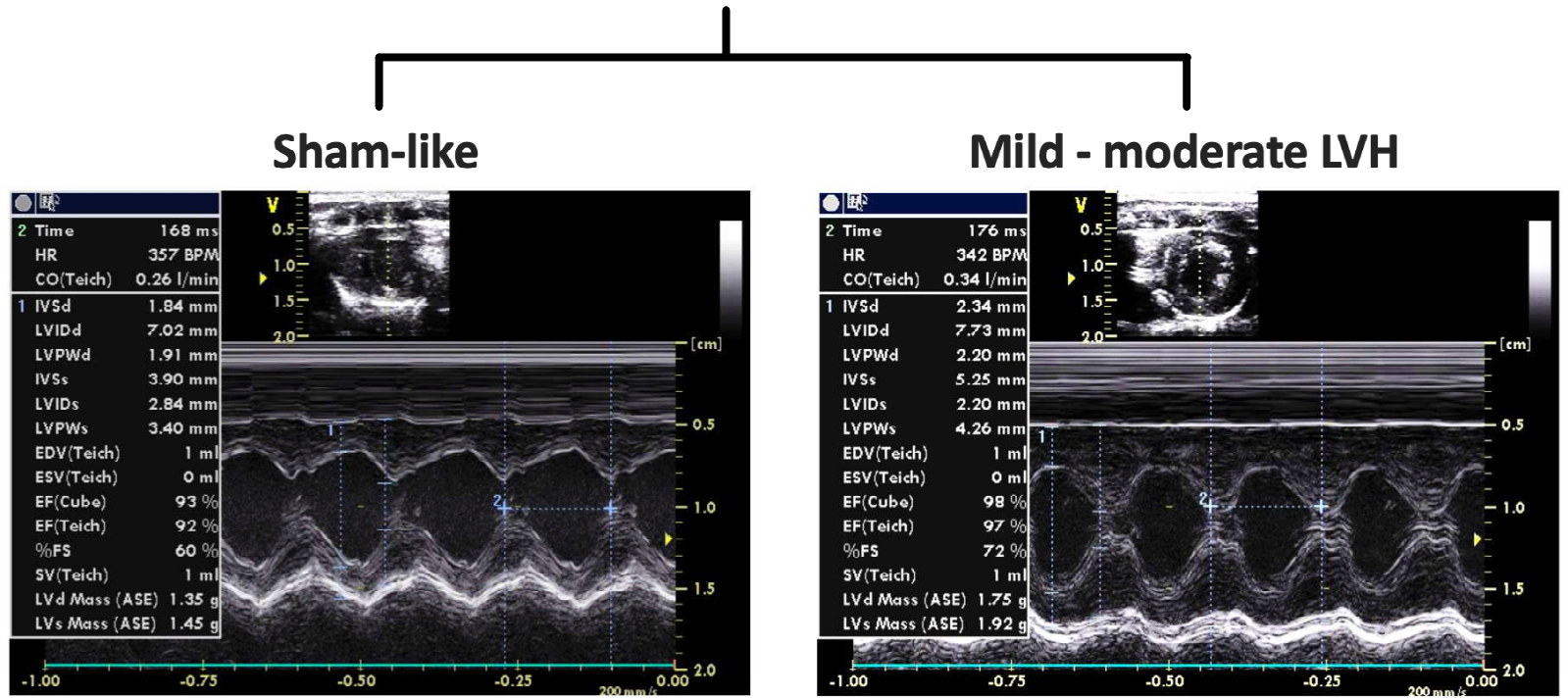
B

Animals that developed severe LVH and severe pressure overload at week 8 post-AAB but remained compensated without significant eccentric remodeling
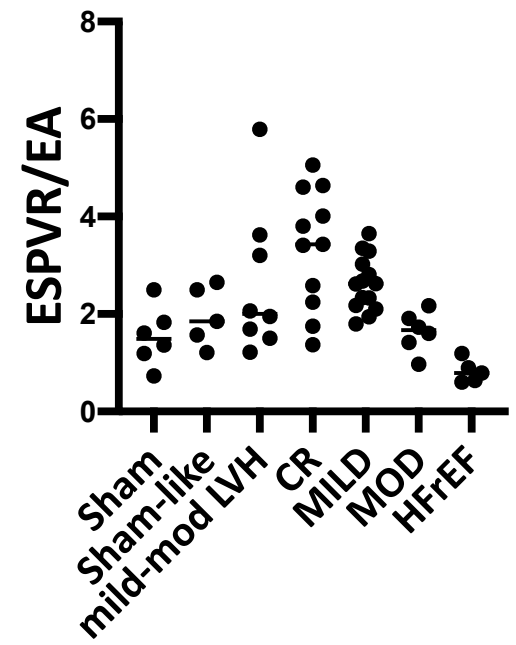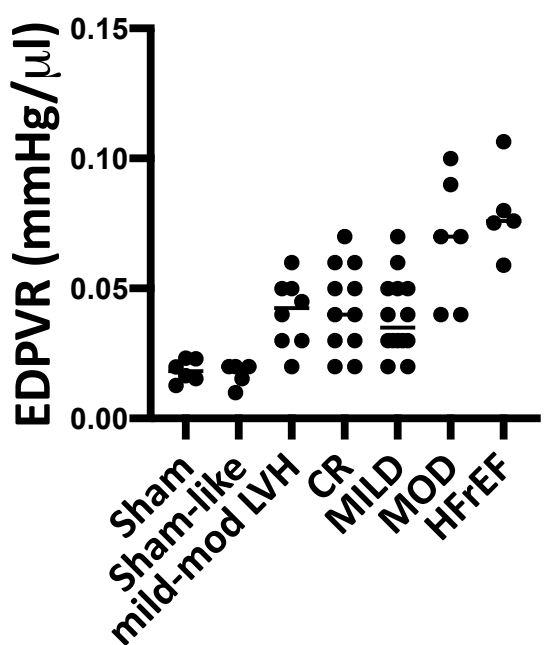
Severe concentric remodeling (CR)   **Severe concentric remodeling and MILD eccentric remodeling**
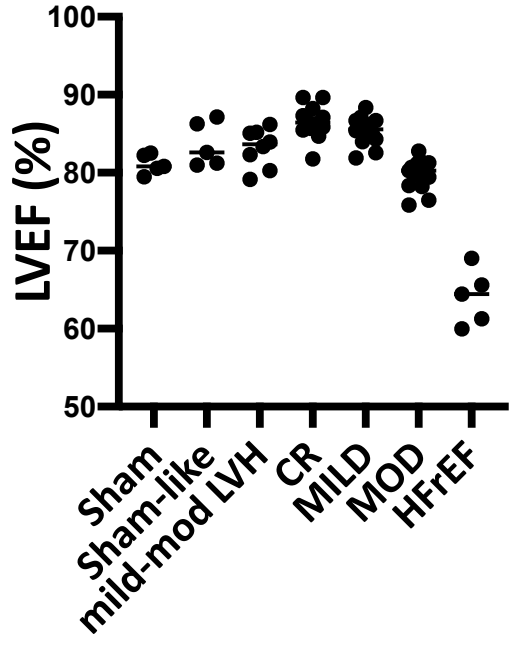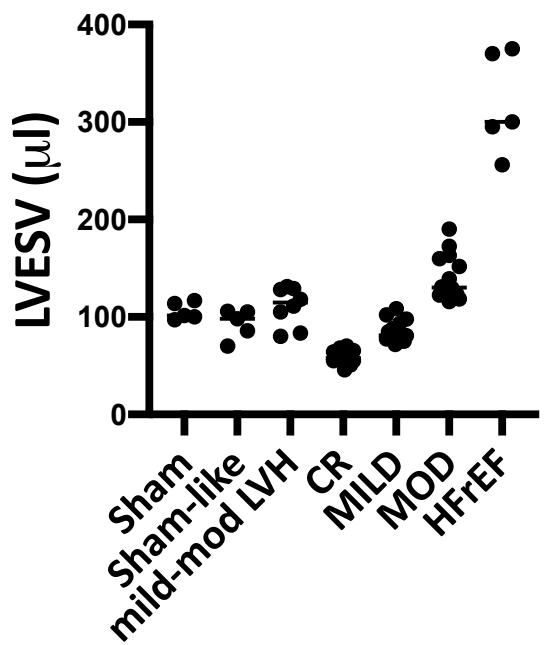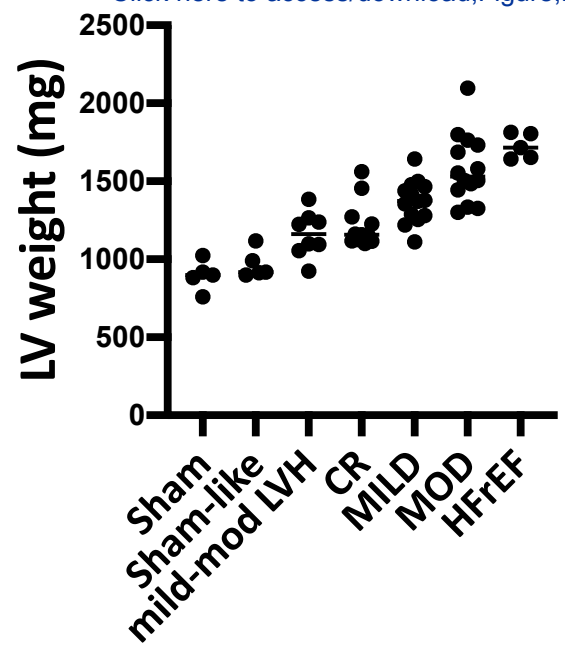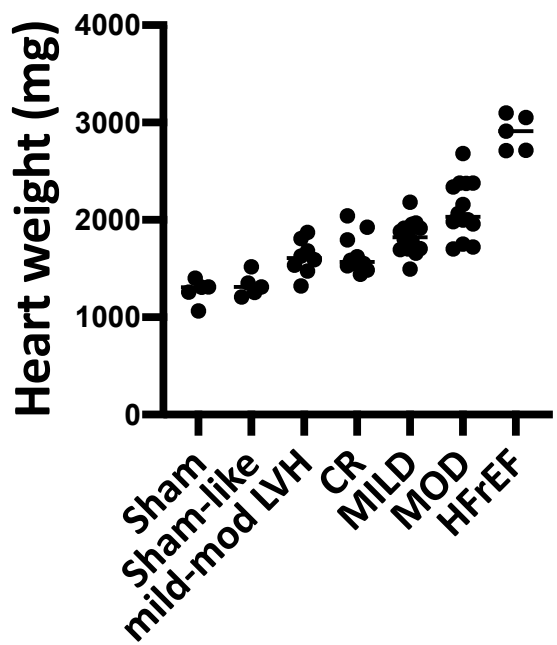
Figure 5
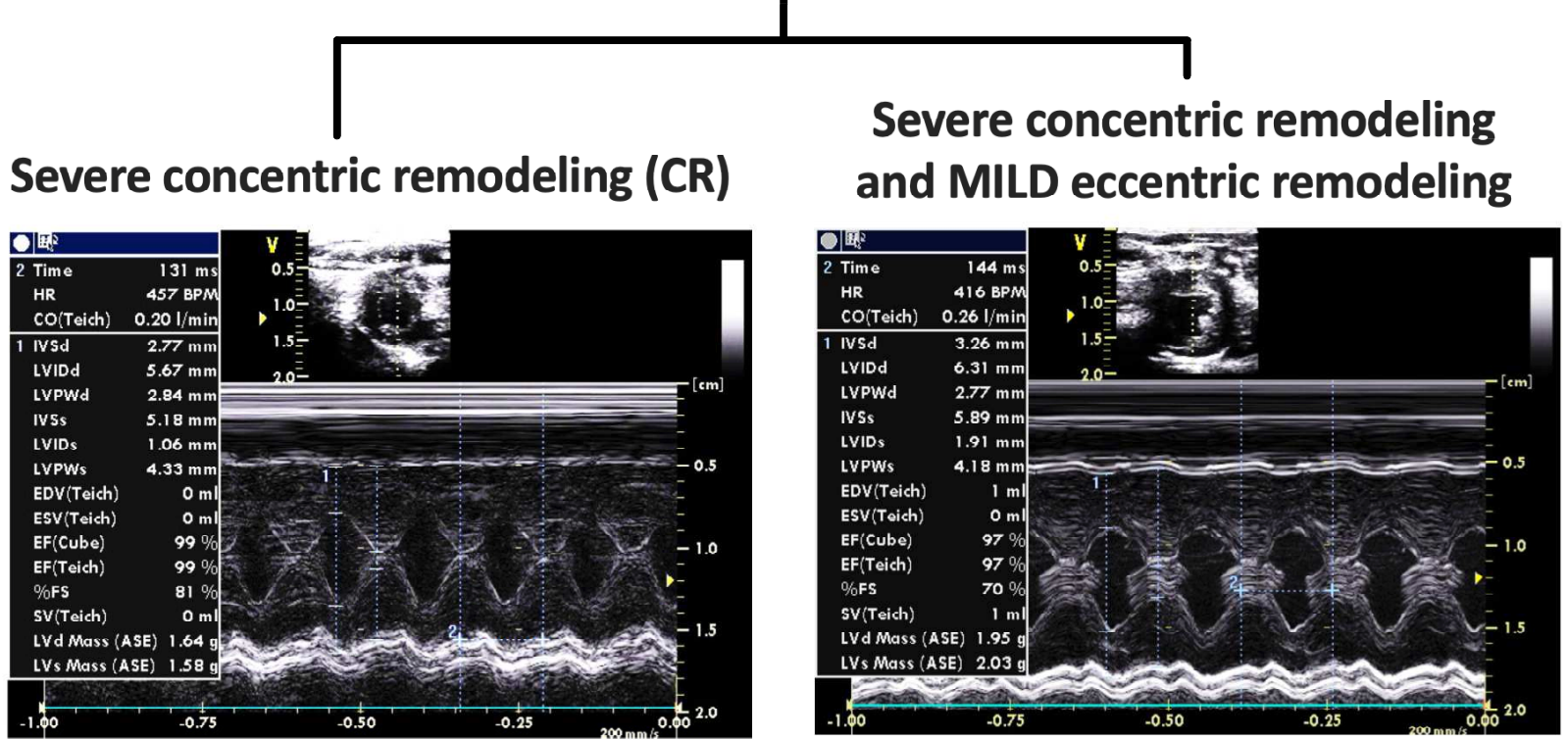
Table 1. Echocardiography and pressure-volume parameters in Sham, Sham-like, Mild-moderate LVH, CR, MILD, MOD and HFrEF phenotypes.

	Sham (n=5)	Sham-like (n=5)	Mild-mod LVH (n=8)	CR (n=11)	MILD (n=14)	MOD (n=14)	HFrEF (n=5)
Body weight (g)	594 ± 37	466 ± 66	464 ± 22	497 ± 43	530 ± 59	478 ± 39	546 ± 18
HW (mg)	1269 ± 124.5	1328 ± 119	1614 ± 177	1645 ± 191a	1821 ± 169a,b	2106 ± 292a,b,c,d,e	2897 ± 182a,b,c,d,e,f
LVW (mg)	897 ± 94	968 ± 91	1161 ± 144	1222 ± 152a	1372 ± 135a,b	1580 ± 219a,b,c,d,e	1726 ± 82a,b,c,d,e
RVW (mg)	218± 22	218 ± 23	266 ± 24	239 ± 26	249 ± 26	283 ± 42a,b	565 ± 76a,b,c,d,e,f
IVSd (cm)	0.19 ± 0.01	0.21 ± 0.01	0.23 ± 0.01a	0.29 ± 0.01a,b,c	0.28 ± 0.02a,b,c	0.28 ± 0.01a,b,c	0.28 ± 0.02a,b,c
LVPWd (cm)	0.20 ± 0.01	0.21 ± 0.02	0.24 ± 0.01a,b	0.29 ± 0.02a,b,c	0.28 ± 0.02a,b,c	0.28 ± 0.01a,b,c	0.30 ± 0.02a,b,c
LVEDV (µl)	560.5 ± 25.8	570 ± 32	668 ± 143	442 ± 42,c	583 ± 45d	697 ± 129d,e	881.5 ± 55.7a,b,c,d,e,f
LVESV (µl)	105.9 ± 8.9	93 ± 15	111 ± 20	59 ± 7a,b,c	85.3 ± 10.6d	139.7 ± 22.5a,b,c,d,e	319.2 ± 51.5a,b,c,d,e,f
LVEF (%)	81.1 ± 1.2	83.7 ± 2.9	83.1 ± 2.5	86.5 ± 2.2a,c	85.4 ± 1.7a	79.8 ± 1.9b,c,d,e	64.1 ± 3.6a,b,c,d,e,f
LVPmax (mmHg)	121 ± 19	126 ± 23	186 ± 23a,b	218 ± 18a,b	221 ± 22a,b,c	*234 ± 25a,b,c	262 ± 16a,b,c,d,e
EDPVR (mmHg/µl)	0.018 ± 0.005	0.017 ± 0.004	0.041 ± 0.013	0.043 ± 0.017	0.039 ± 0.015	*0.068 ± 0.025a,b,c,d,e	0.079 ± 0.017a,b,c,d,e
ESPVR/EA	1.57 ± 0.67	1.96 ± 0.61	2.63 ± 1.52	3.35 ± 1.23a	2.62 ± 0.55	*1.63 ± 0.41d	0.82 ± 0.24c,d,e

Data are presented as mean ± standard deviation. Statistical analysis was performed using One-way ANOVA. P < 0.05 was considered significant.

aP < 0.05 vs Sham
bP < 0.05 vs Sham-like
cP < 0.05 vs Mild-modearte LVH
dP < 0.05 vs CR
eP < 0.05 vs MILD
fP < 0.05 vs MOD
***n=6**

Abbreviations: HW: heart weight, LVW: left ventricular weight, RVW: right ventricular weight, IVSd: septal wall thickness in diastole, LVPWd: left ventricular posterior wall thickness in diastole. LVEDV: left ventricular end-diastolic volume, LVESV: left ventricular end-systolic volume, LVEF: left ventricular ejection fraction, LVPmax: left ventricular maximal pressure, EDPVR: end-diastolic pressure volume relationship, ESPVR: end-systolic pressure volume relationship, EA: arterial elastance.

Name of Reagent/ Equipment	Company	Catalog Number	Comments/Description
Adson forceps	F.S.T.	11019-12	surgical tool
Alm chest retractor with blunt teeth	ROBOZ	RS-6510	surgical tool
Graefe forceps, curved	F.S.T.	11152-10	surgical tool
Halsted-Mosquito Hemostats, straight	F.S.T.	13010-12	surgical tool
Hardened fine iris scissors, straight	Fine Science Tools F.S.T.	14090-11	surgical tool
hemoclip traditional-stainless steel ligating clips	Weck	523435	surgical tool
Mayo-Hegar needle holder	F.S.T.	12004-18	surgical tool
mechanical ventilator	CWE inc	SAR-830/AP	mechanical ventilator for small animals
Weck stainless steel Hemoclip ligation	Weck	533140	surgical tool

Response to Editors and Reviewers Comments

Response to Editors Comments

1. **Please take this opportunity to thoroughly proofread the manuscript to ensure that there are no spelling or grammar issues.**

We thank the editors for their comment. We have carefully proofread the manuscript.

2. Unfortunately, there are a few sections of the manuscript that show significant overlap with previously published work. Though there may be a limited number of ways to describe a technique, please use original language throughout the manuscript. Please revise the entire first paragraph in the Introduction.

The first paragraph in the introduction section has been entirely revised.

3. Please obtain explicit copyright permission to reuse any figures from a previous publication. Explicit permission can be expressed in the form of a letter from the editor or a link to the editorial policy that allows re-prints. Please upload this information as a .doc or .docx file to your Editorial Manager account. The Figure must be cited appropriately in the Figure Legend, i.e. "This figure has been modified from [citation]."

We have obtained copyright permission for images and figures that were used in previous publications. Specifically:

a- Figure 1A: Representative 2D M-mode echo images of Sham (figures 1A and 4A) and MOD phenotypes were used from fig 5A of previously published work "Chaanine et al, AJP: Heart and Circ physiology 2016". As per APS journals policy: "authors may republish parts of their final-published work (e.g., figures, tables), without charge and without requesting permission, provided that full citation of the source is given in the new work".

b- Figure 1B and 1C: Vascular clip images were used from fig 1A of previously published work "Chaanine et al, Methods in Molecular Biology 2018". Copyright permission from Springer Nature to reuse the published was obtained.

c- Figure 3: Pressure volume loop tracing were used from figs 1F, 2D and 3D of previously published work "Chaanine et al, Circ HF 2013". As per AHA Journals policies under "permission and rights", it is stated that: "Authors may use parts of the work (eg, tables, figures) in subsequent works without requesting permission from the AHA".

d- Figure 4B: Representative 2D M-mode echo images of CR and MILD phenotypes were used from fig 2A of previously published work "Chaanine et al, JAHA 2017". Similarly, as per AHA Journals policies under "permission and rights", it is stated that: "Authors may use parts of the work (eg, tables, figures) in subsequent works without requesting permission from the AHA".

Above information has been uploaded to the Editorial Manager account in a word document titled: "Copyright Permission to Reuse Previously Published Work".

The figure legends of figures 1, 3 and 4 have been updated to reflect the citation of figures obtained from previously published work.

4. Please add a one-line space between each of your protocol steps.

We have added a one-line space between each of the protocol steps and notes.

5. Step 1.1-1.11: Please write each step in the imperative tense.

We have done so.

6. Please avoid long steps/notes (more than 4 lines).

Steps that were longer than 4 lines were divided into subsequent steps.

Notes that were longer than 4 lines were divided into two or more notes.

7. Figure 3: Please add a short description of the figure in Figure Legend.

We have added a short description of figure 3 to figure 3 legend and as suggested by Reviewer#2.

8. Please do not abbreviate journal titles for references.

We have corrected and replaced abbreviated journal title with full journal name/title.

<u>**Response to Reviewers Comments**</u>

Reviewer #1

Major Concerns:

The Introduction ends abruptly and it is not clear what is proposed with this model. By reading the introduction at first, I thought that modifications proposed here would lead to a reproducible way to create moderate (MOD) PO rat model. It does not seem to be the case.

We have done modification of clip size to achieve the MOD phenotype. This is what we intended to describe here and we hoped that all animals would develop the MOD phenotype. However, unfortunately, this is not the case despite that all animals subjected to AAB have the same clip size. This is in a way unavoidably frustrating, as one have to acknowledge the fact that variations are seen in biology and are related to intrinsic (degree of hypertrophy in response to pressure overload) and extrinsic (injury and remodeling of the ascending aorta around the clip) factors. These biological variations in response to an existing stressor are seen in both animals and humans.

We have significantly revised the introduction section of the manuscript and added a paragraph at the end to elaborate on the advantage of the MOD phenotype over the HFrEF phenotype and to highlight the purpose of the manuscript.

Methodology is well described for one major exception in my opinion. The paragraph describing the calibration of the clips to obtain the desired area is difficult to understand. A figure would be useful. I understand that a video will eventually be added but this part is not clear in the text.

We thank the reviewer for his/her comment. The calibration of the vascular device to obtain a specific clip size of interest will be clarified in the video that will be obtained and added at a later time.

I was wondering if the description of how LV volumes were estimated should be included in the Methods and not in the Results section.

We had similar thoughts, but because it is too lengthy to describe how to calculate LV volumes in the "protocol" section, we opted to describe this in the results section and reference the figure (figure 2) illustrating how to measure LV length and area in diastole and systole from the 2D long and short parasternal axis echo images, respectively, in order to calculate LV volumes.

Results section should make one point clearer. My understanding is that the 1.5mm2 clip leads to more severe phenotypes than the 2 mm2 clip but I had wished that some

of the figures (or tables) would illustrate how the parameters measured are related to clip size.

We thank the reviewer for his/her comment. As stated above and in the introduction section, variations in response to pressure overload are seen even if the same clip size is used. The figures are illustrating the different phenotypes that are encountered and how to differentiate by echocardiography between the phenotypes of interest (MOD and HFrEF) versus other encountered phenotypes that fail to develop severe PO and LVH or that develop severe PO and concentric LVH but without significant eccentric remodeling. Figure 1B is showing the clip size to obtain MOD phenotype, whereas the HFrEF phenotype is only encountered by a clip size of 1.5 mm^2, figure 1C. However, not all animals subjected to this clip size will develop the MOD or HFrEF phenotype. Also, there is no way to predict findings or parameters related to clip size and which animals are going to develop MOD or HFrEF phenotype at the time when the animals are fully compensated (week 3 post-AAB).

The authors failed to discuss other banding models in the rat and how their model constitutes an improvement.

We have addressed this at the end of the discussion section. Revision and additions made are highlighted in the "tracked changes" file.

The authors should concentrate less on how to make an echo exam in rats and more about the evolution of their model.

We have addressed this in the introduction and in the discussion part of the manuscript.

Minor Concerns:
I suppose some statistical analysis was made but I did not find it in the methods.

The format of the manuscript does not allow for a method section. That is why we opted to describe the statistical analysis in the footnote section of table 1.

Reviewer #2

Major Concerns:

In the last paragraph of the introduction instead of comparing with myocardial infarction, the author should compare with results in spontaneously hypertensive rats.

We thank the reviewer for his/her comment. The reason we compared the PO-induced HF model produced by AAB with the MI model and not the SHR model is that the SHR and other models of hypertension, such as DOCA salt, are mainly used to investigate mechanisms and therapies related to hypertension and possibly diastolic dysfunction,

more so than HFrEF and myocardial eccentric remodeling (*Doggrell* et al. *Cardiovascular Research* 39 (1998) 89–105). Moreover, it takes about two years for the SHR to develop systolic HF and mechanism of systolic HF is not entirely known and is confounded by aging. Also, the increase in afterload and myocardial wall stress in systole in the SHR is nowhere close to that seen with the PO-induced HF model. We have highlighted these differences between the SHR and PO-induced HF models at the end of the discussion section of the manuscript.

Additionally the introduction should clarify what is the aim of the article (to detail a procedure?).

We have now clarified this in the last paragraph of the introduction section.

Finally, and I might be wrong, because a lot of images has been used already in the author's previous publications, it might be important to check the copyright issue.

Copyright permission to use previously published work has been addressed and obtained.

Minor Concerns:
In figure 1, replace "desired" by representative

Change has been made as suggested by the reviewer.

In figure 3 legend, add a succinct method to obtain PV loop.

Change has been made as suggested by the reviewer.

Because in the author's 2017 publication the data refers to 3 weeks post AAB, the author should be consistent with it.
We thank the reviewer for his/her comment. There is no significant difference in echocardiographic findings between week 2 and week 3 post-AAB. We have stated this in the discussion section, first paragraph. As per reviewer's request we have changed week 2 to week 3 and revised this in the body of the manuscript and figure legends when needed.

Similarly the dosage of ketamine and xylazine is different than in the 2017 publication.

We have corrected Ketamine and Xylazine dose in the manuscript to reflect similar information in previous publications: Ketamine 65 mg/kg and Xylazine 5 mg/kg.

I imagine the format of table 1 is a mistake.

The format of table 1 has been modified to fit in one page. The journal instruction is to provide the table in an excel, .xlsx, file.

Reviewer #3

Major:
According to our experience, 20% success rate seems to be very low, and raises the question of harm/benefit in animal studies. It should be at least 40% after proper settings of anesthesia and surgical circumstances, as well as choosing the right animal size.

Severe pressure overload and concentric LVH is achieved in over 60% of banded animals at week 8 after ascending aortic banding. However, The MOD phenotype is seen in only 20% of the totally banded animals at week 8 post AAB or in 33% of the animals with severe pressure overload and concentric LVH. We experienced higher postoperative mortality when Isoflurane was used. Moreover, we have tried to band animals using a weight range between 80 – 200 g and similar results were seen. Banding animals with weight greater than 200g was associated with a higher postoperative mortality.

Anesthetics: the combination of Ketamine and Xylazine (K/X) has negative effect on cardiac function (doi: 10.3892/etm.2013.1213), especially in stages with acute overload of the heart (e.g. this setting). Why have the Authors chosen this kind of anesthetics? This side-effect might severely affect the periprocedural mortality of these animals. Moreover, please provide proper initial dose - not ranges - for the reproducibility of these experiments.

As stated above, we experienced higher perioperative mortality with Isoflurane compared to Ketamine and Xylazine.

Ketamine dose was changed to 65 mg/kg and Xylazine was changed to 5 mg/kg.

What about temperature of the animal? Which range of temperature is allowed during the operation and afterwards. This is also a critical question as K/X anesthesia causes already severe heart rate depression.

We use a heating pad and cover the animal after finishing the procedure until it recovers from anesthesia. We do not see significant fluctuation in body temperature when using a rectal probe, 37°C ± 1°C, as the procedure is quick to perform and takes about 10-15 minutes from start to end. Most animals recover from anesthesia shortly, about 10 – 15 minutes, after the procedure is finished and are then returned to the cage.

Table 1. has been cut into four pages, however as one can see, there is no alteration of EF and contractility in MOD group compared to Sham animals.

Despite that the LVEF is the same between Sham and MOD phenotype, LV end diastolic volumes and LV end systolic volumes are significantly higher in the MOD phenotype compared to Sham due to eccentric remodeling.

The contractility in the MOD is lower than Sham if you correct for the V_0 (this has been mentioned and clarified in the last paragraph of the results section). Because of the PO, the end-systolic pressure is significantly higher and the V_0 is significantly shifted to the right in the MOD phenotype compared to Sham; thus giving a false impression of similar contractility (Ees slope) when compared to Sham. In my opinion the contractility of the MOD phenotype should be compared to the contractility of the CR phenotype as both phenotypes have similar degree of PO and given that the CR phenotype remained compensated at week 8 post-AAB compared to week 3 post-AAB. It is then that one could appreciate the decline in contractility of the MOD phenotype at week 8 post-AAB compared to when these animals were fully compensated at week 3 post-AAB.

Copyright Permission from Journals/Publisher to Reuse Previously Published Work.

Permission/Policy from APS journals:

brought to you by Tulane University

🏠 | JOURNALS ⌄

Copyright and Permissions

Reuse by Authors of Their Work Published by APS

Reuse by Non-authors of APS Published Content

Reuse in APS Publications of non-APS Published Content

Reuse by Authors of Their Work Published by APS

The APS Journals are copyrighted for the protection of authors and the Society. The Mandatory Submission Form serves as the Society's official copyright transfer form. Author's rights to reuse their APS-published work are described below:

Republication in New Works	Authors may republish parts of their final-published work (e.g., figures, tables), without charge and without requesting permission, provided that full citation of the source is given in the new work.
Meeting Presentations and Conferences	Authors may use their work (in whole or in part) for presentations (e.g., at meetings and conferences). These presentations may be reproduced on any type of media in materials arising from the meeting or conference such as the proceedings of a meeting or conference. A copyright fee will

Permission from Springer Nature: pertaining to the previously published work in the Methods in Molecular Biology Journal.

SPRINGER NATURE LICENSE
TERMS AND CONDITIONS

Dec 19, 2019

This Agreement between Tulane University School of Medicine -- Antoine Chaanine ("You") and Springer Nature ("Springer Nature") consists of your license details and the terms and conditions provided by Springer Nature and Copyright Clearance Center.

License Number	4732621436607
License date	Dec 19, 2019
Licensed Content Publisher	Springer Nature
Licensed Content Publication	Springer eBook
Licensed Content Title	Characterization of the Differential Progression of Left Ventricular Remodeling in a Rat Model of Pressure Overload Induced Heart Failure. Does Clip Size Matter?
Licensed Content Author	Antoine H. Chaanine, Roger J. Hajjar
Licensed Content Date	Jan 1, 2018
Type of Use	Journal/Magazine
Requestor type	academic/university or research institute

Is this reuse sponsored by or associated with a pharmaceutical or a medical products company?	no
Format	print and electronic
Portion	figures/tables/illustrations
Number of figures/tables/illustrations	1
Will you be translating?	no
Circulation/distribution	1000 - 1999
Author of this Springer Nature content	yes
Title of new article	Characterization of the Differential Progression of Left Ventricular Remodeling in a Rat Model of Pressure Overload Induced Heart Failure. Does Clip Size Matter?
Lead author	Antoine Chaanine
Title of targeted journal	Journal of Visualized Experiments
Publisher	MyJove Corp
Expected publication date	Feb 2020
Portions	Vascular clip images from figure 1A

	Tulane University School of Medicine
Requestor Location	1430 Tulane Avenue
	Heart and Vascular Institute
	NEW ORLEANS, LA 70112
	United States
	Attn: Tulane University School of Medicine

Total	0.00 USD

Terms and Conditions

Springer Nature Customer Service Centre GmbH
Terms and Conditions

This agreement sets out the terms and conditions of the licence (the **Licence**) between you and **Springer Nature Customer Service Centre GmbH** (the **Licensor**). By clicking 'accept' and completing the transaction for the material (**Licensed Material**), you also confirm your acceptance of these terms and conditions.

1. Grant of License

1. 1. The Licensor grants you a personal, non-exclusive, non-transferable, world-wide licence to reproduce the Licensed Material for the purpose specified in your order only. Licences are granted for the specific use requested in the order and for no other use, subject to the conditions below.

1. 2. The Licensor warrants that it has, to the best of its knowledge, the rights to license reuse of the Licensed Material. However, you should ensure that the material you are requesting is original to the Licensor and does not carry the copyright of another entity (as credited in the published version).

1. 3. If the credit line on any part of the material you have requested indicates that it was reprinted or adapted with permission from another source, then you should also seek permission from that source to reuse the material.

2. Scope of Licence

2. 1. You may only use the Licensed Content in the manner and to the extent permitted

by these Ts&Cs and any applicable laws.

2. 2. A separate licence may be required for any additional use of the Licensed Material, e.g. where a licence has been purchased for print only use, separate permission must be obtained for electronic re-use. Similarly, a licence is only valid in the language selected and does not apply for editions in other languages unless additional translation rights have been granted separately in the licence. Any content owned by third parties are expressly excluded from the licence.

2. 3. Similarly, rights for additional components such as custom editions and derivatives require additional permission and may be subject to an additional fee. Please apply to Journalpermissions@springernature.com/bookpermissions@springernature.com for these rights.

2. 4. Where permission has been granted **free of charge** for material in print, permission may also be granted for any electronic version of that work, provided that the material is incidental to your work as a whole and that the electronic version is essentially equivalent to, or substitutes for, the print version.

2. 5. An alternative scope of licence may apply to signatories of the STM Permissions Guidelines, as amended from time to time.

3. Duration of Licence

3. 1. A licence for is valid from the date of purchase ('Licence Date') at the end of the relevant period in the below table:

Scope of Licence	Duration of Licence
Post on a website	12 months
Presentations	12 months
Books and journals	Lifetime of the edition in the language purchased

4. Acknowledgement

4. 1. The Licensor's permission must be acknowledged next to the Licenced Material in print. In electronic form, this acknowledgement must be visible at the same time as the figures/tables/illustrations or abstract, and must be hyperlinked to the journal/book's homepage. Our required acknowledgement format is in the Appendix below.

5. Restrictions on use

5. 1. Use of the Licensed Material may be permitted for incidental promotional use and minor editing privileges e.g. minor adaptations of single figures, changes of format, colour and/or style where the adaptation is credited as set out in Appendix 1 below. Any other changes including but not limited to, cropping, adapting, omitting material that affect the meaning, intention or moral rights of the author are strictly prohibited.

5. 2. You must not use any Licensed Material as part of any design or trademark.

5. 3. Licensed Material may be used in Open Access Publications (OAP) before publication by Springer Nature, but any Licensed Material must be removed from OAP sites prior to final publication.

6. Ownership of Rights

6. 1. Licensed Material remains the property of either Licensor or the relevant third party and any rights not explicitly granted herein are expressly reserved.

7. Warranty

IN NO EVENT SHALL LICENSOR BE LIABLE TO YOU OR ANY OTHER PARTY OR ANY OTHER PERSON OR FOR ANY SPECIAL, CONSEQUENTIAL, INCIDENTAL OR INDIRECT DAMAGES, HOWEVER CAUSED, ARISING OUT OF OR IN CONNECTION WITH THE DOWNLOADING, VIEWING OR USE OF THE MATERIALS REGARDLESS OF THE FORM OF ACTION, WHETHER FOR BREACH OF CONTRACT, BREACH OF WARRANTY, TORT, NEGLIGENCE, INFRINGEMENT OR OTHERWISE (INCLUDING, WITHOUT LIMITATION, DAMAGES BASED ON LOSS OF PROFITS, DATA, FILES, USE, BUSINESS OPPORTUNITY OR CLAIMS OF THIRD PARTIES), AND
WHETHER OR NOT THE PARTY HAS BEEN ADVISED OF THE POSSIBILITY OF SUCH DAMAGES. THIS LIMITATION SHALL APPLY NOTWITHSTANDING ANY FAILURE OF ESSENTIAL PURPOSE OF ANY LIMITED REMEDY PROVIDED HEREIN.

8. Limitations

8. 1. ***BOOKS ONLY****:*Where **'reuse in a dissertation/thesis'** has been selected the following terms apply: Print rights of the final author's accepted manuscript (for clarity, NOT the published version) for up to 100 copies, electronic rights for use only on a personal website or institutional repository as defined by the Sherpa guideline (www.sherpa.ac.uk/romeo/).

9. Termination and Cancellation

9. 1. Licences will expire after the period shown in Clause 3 (above).

9. 2. Licensee reserves the right to terminate the Licence in the event that payment is not received in full or if there has been a breach of this agreement by you.

Appendix 1 — Acknowledgements:

For Journal Content:
Reprinted by permission from [**the Licensor**]: [**Journal Publisher** (e.g. Nature/Springer/Palgrave)] [**JOURNAL NAME**] [**REFERENCE CITATION** (Article name, Author(s) Name), [**COPYRIGHT**] (year of publication)

For **Advance Online Publication papers:**
Reprinted by permission from [**the Licensor**]: [**Journal Publisher** (e.g. Nature/Springer/Palgrave)] [**JOURNAL NAME**] [**REFERENCE CITATION** (Article name, Author(s) Name), [**COPYRIGHT**] (year of publication), advance online publication, day month year (doi: 10.1038/sj.[JOURNAL ACRONYM].)

For Adaptations/Translations:
Adapted/Translated by permission from [**the Licensor**]: [**Journal Publisher** (e.g. Nature/Springer/Palgrave)] [**JOURNAL NAME**] [**REFERENCE CITATION** (Article name, Author(s) Name), [**COPYRIGHT**] (year of publication)

Note: For any republication from the British Journal of Cancer, the following credit line style applies:

Reprinted/adapted/translated by permission from [**the Licensor**]: on behalf of Cancer Research UK: : [**Journal Publisher** (e.g. Nature/Springer/Palgrave)] [**JOURNAL NAME**] [**REFERENCE CITATION** (Article name, Author(s) Name), [**COPYRIGHT**] (year of publication)

For **Advance Online Publication** papers:

Reprinted by permission from The [**the Licensor**]: on behalf of Cancer Research UK: [**Journal Publisher** (e.g. Nature/Springer/Palgrave)] [**JOURNAL NAME**] [**REFERENCE CITATION** (Article name, Author(s) Name), [**COPYRIGHT**] (year of publication), advance online publication, day month year (doi: 10.1038/sj. [JOURNAL ACRONYM])

For Book content:
Reprinted/adapted by permission from [**the Licensor**]: [**Book Publisher** (e.g. Palgrave Macmillan, Springer etc) [**Book Title**] by [**Book author**(s)] [**COPYRIGHT**] (year of publication)

Other Conditions:

Version 1.2

Questions? customercare@copyright.com or +1-855-239-3415 (toll free in the US) or +1-978-646-2777.

[AHA/ASA Journals](#)

AHA/ASA Journal Policies

- [Submission Requirements](#)
- [Research Guidelines](#)
- [Figure Guidelines](#)
- [TOP Guidelines](#)
- [Prior Publication Policy](#)
- [Open Access Information](#)
- [Public Access Policy](#)
- [Permissions and Rights](#)
- [Embargo Policy](#)
- [Conflict of Interest Procedures](#)
- [Ethical Conduct Policy](#)

Permissions and Rights FAQ

Authors of submitted manuscripts in American Heart Association jour nals are required to sign a Authorship Responsibility and Copyright Transfer Agreement (CTA) or Open Access (OA) Licensing Agreement. More information on the AHA's Open Access policy can be found online [here](#). The following pertains to authors who intend to sign a CTA or request permission from an AHA copyrighted article:

Q—*Where can I find the CTA?*

acceptance, please contact the Publisher (Wolters Kluwer Health/Lippincott Williams & Wilkins) at PE-AHAJournal@wolterskluwer.com.

Q—*Can I reuse my figures and tables in future works without asking permission?*
A—Yes. The current CTA states "Authors may use parts of the work (eg, tables, figures) in subsequent works without requesting permission from the AHA."

Q—*Can I make copies of my article for my lectures, classroom teaching, and other educational use?*
A—Yes, provided you cite the original source and copyright notice. See also "Fair Use of Copyrighted Materials" (section 107, title 17, US Code)

Q—*I want to use figures or tables or other content from an AHA journal, but I am not an author of the original article.*
A—Permission requests are handled **online** via RightsLink, a service of the Copyright Clearance Center. Steps to request permission are:

Go to the **online version** of the AHA journal article for which you are requesting permission.
Locate the "Request Permissions" link in the menu in the middle column of the Web page (under "Article Tools").
A new window opens, which is Rightslink.
Follow the step-by-step instructions for requesting permission
1. selecting the way the content will be used
2. creating an account, if one does not exist already
3. accepting the terms and conditions for reuse
4. method of payment.

For AHA Scientific Statements and Guidelines, permission to reprint, modify, alter, enhance, copy, or distribute this content must be obtained from the American Heart Association. Instructions are located at Heart.org. View the copyright permission guidelines. A link to the "Copyright Permissions Request Form" appears on the right side of the Web page.